

# Electrical resistivity of copper reinforced with short carbon fibres

A. F. WHITEHOUSE, C. M. WARWICK\*, T. W. CLYNE

*Department of Materials Science and Metallurgy, Pembroke Street, Cambridge CB2 3QZ, UK*

The electrical resistivity of copper reinforced with short aligned carbon fibres has been measured in axial and transverse directions as a function of fibre content. The results have been considered in the light of predictions from the Eshelby equivalent homogeneous inclusion method for modelling of conduction. Higher resistivities, particularly for transverse current flow, were observed than is predicted on the basis of an isotropic matrix resistivity equal to that of unreinforced copper. This is thought to be explicable in terms of the effect of relatively high levels of elongated porosity present in the specimens examined.

## 1. Introduction

Potential areas of application for metal matrix composites (MMCs) include those requiring a combination of good mechanical properties with high electrical and/or thermal conductivity. For example, it may be possible by introducing strong, stiff fibres into a highly conductive matrix to achieve improvements in yield stress and work hardening rate at lower cost in impaired conductivity than is possible by conventional alloying operations. In order to explore such possibilities, a sound theoretical basis is required for prediction of the conductivity of such composites.

A number of models have been developed for conduction in composites [1-5]. Many of these are oriented towards long fibre composites. The axial conductivity of an aligned long fibre composite should be given by a (Voigt) Rule of Mixtures, but more complex expressions are needed for the transverse conductivity, particularly if the fibres are carrying any current. For short fibres and/or a degree of fibre misorientation, the Eshelby equivalent homogeneous inclusion method, developed for conduction by Taya and co-workers [6-8], is proving a versatile tool for prediction of composite transport properties. The effect of a finite interfacial contact resistance can also be incorporated by introducing a thin coating of specified conductivity on to the fibres [7]. An Eshelby-type model is not well suited to insulating matrix/conducting fibre composites at low fibre volume fraction, where a percolation-type model is more appropriate [9, 10]. However, for a conducting matrix, the Eshelby method should be reliable over a wide range of fibre volume fraction. In the vast majority of MMC systems, the reinforcement can be taken as electrically (but not necessarily thermally [11]) insulating. There is not normally, therefore, any concern about interfacial electrical resistance.

There have been a few reported studies of the electrical properties of MMCs [12-14]. Abukay *et al.*

[12] examined aluminium reinforced with 60% continuous boron fibres and found anomalously high transverse resistivities. They attributed this to scattering of electrons by the fibre/matrix interface when current flow is transverse. In fact, this seems a little unlikely (particularly with such coarse fibres), as the mean free path between collisions in metals is short (approximately a few tens or hundreds of atomic diameters) and extra scattering events separated by distances several orders of magnitude greater than this are unlikely to have any effect.

A discontinuous MMC was examined by DeBont *et al.* [14], who measured conductivities of sintered compacts made from a mixture of conducting and insulating powders. They presented a simple numerical model, but this was really aimed at exploring the percolation threshold for low volume fractions of conducting constituent; no information was given about microstructure or conduction paths.

In the present work, the resistivity of a short fibre MMC is measured as a function of fibre content and the results compared with predictions from the Eshelby model, with the objective of identifying the significance of microstructural variables.

## 2. Experimental procedure

### 2.1. Composite production

Composites were made by ball milling a mixture of copper powder ( $\sim 50 \mu\text{m}$  diameter) and carbon fibre ( $7 \mu\text{m}$  diameter, chopped into lengths of about 10 mm), followed by transfer to a copper can, which was evacuated and sealed by electron beam welding. The can was then preheated to  $850^\circ\text{C}$  and extruded in a die with a semi-angle of  $45^\circ$  and an extrusion ratio of 14.4. After extrusion to a cylindrical bar of diameter 22 mm, the can material was machined from the extrudate. Courtaulds LXA293A fibre was used, which is

\* Present address: BP Research Centre, Chertsey Road, Sunbury on Thames, Middlesex, UK.

quoted by the manufacturer as having axial and transverse electrical resistivities of 1400 and 700  $\mu\Omega$  cm, respectively. These values (and those of all other carbon fibres, some of which were used in small quantities within the current programme) are effectively infinite in comparison with that of copper ( $\sim 2 \mu\Omega$  cm). Composites were made up with 7%, 14%, 20% and 30% by volume of fibre.

## 2.2. Electrical measurements

The composites, and extruded specimens of unreinforced copper, were machined into the form of thin strips, with the longest dimension either parallel or transverse to the extrusion direction. These were then placed in a special jig for making the electrical connections, which is illustrated in Fig. 1. An a.c. circuit was used for the measurements. The circuit diagram is

shown in Fig. 2. A fixed current (1 A in this case) is passed through the specimen via two crocodile clips, modulated at a constant frequency of 1 kHz. The potential drop across the specimen between the two spring-loaded probes, from which the resistivity of the material can be deduced, is then amplified and measured. In making this measurement, the potential drop across other resistances in the sensing circuit must be eliminated. This drop generates an offset in the mean voltage of the a.c. signal. This d.c. offset is removed by passing the signal through an a.c. amplifier, after which it is rectified by a demodulator and then passed through an integrator to remove noise and finally displayed as a d.c. voltage ( $\sim 100 \mu\text{V}$  for these specimens).

The dimensions of the specimens were measured using a micrometer, with the average of several readings of width and thickness being taken along the length of the strip. The distance between the probes

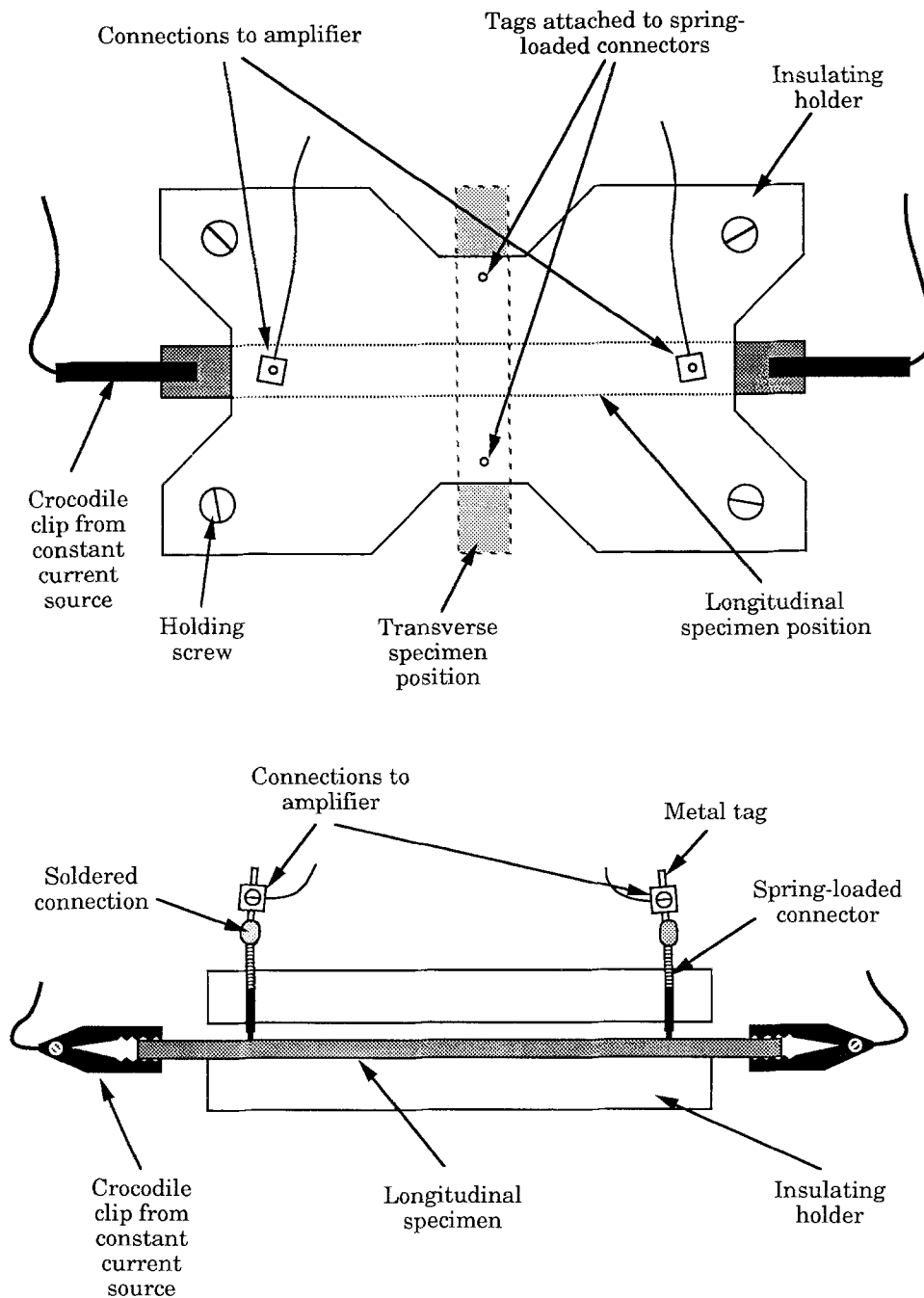


Figure 1 Schematic illustration of the jig for specimen support during electrical measurements.

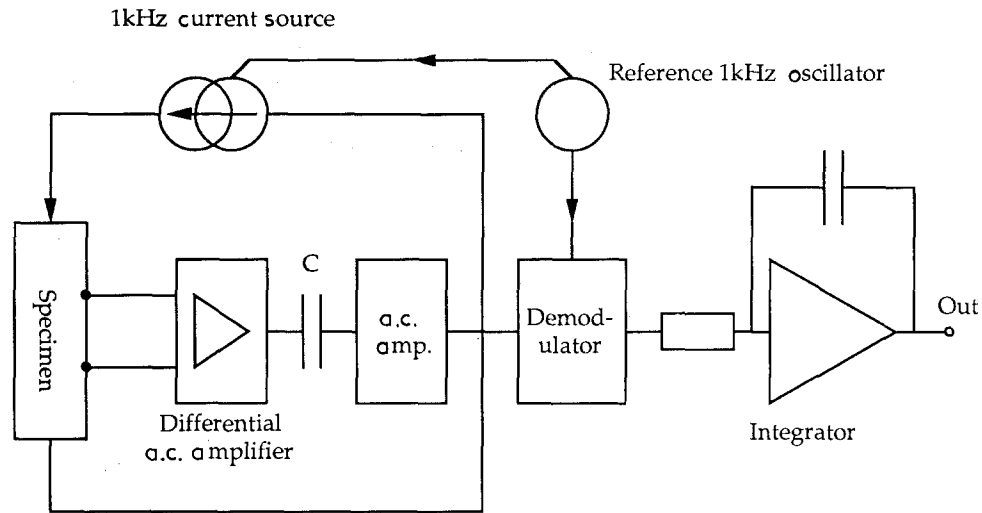


Figure 2 Circuit diagram for arrangement used in electrical measurements.

was about 23 and 6 mm for longitudinal and transverse specimens, respectively. The multimeter was zeroed, with no current through the specimen, before each reading and checked for zero drift after each measurement. Twenty readings were taken for each specimen, with its position in the jig being reversed after ten readings. It was found that the two sets of

readings were always approximately the same, implying no asymmetry of the contact resistances.

### 2.3. Microstructural characterization

Specimens were polished flat and examined in the optical microscope. Some were also deep etched using concentrated nitric acid, for examination in the scanning electron microscope. Fibre aspect ratio measurements cannot be made on polished sections because of uncertainties about the effect of fibre misalignment and so this was studied on extracted fibres. Small specimens were dissolved in concentrated nitric acid and the resulting suspension of fibres was then diluted with water. This mixture was then agitated and fibres were allowed to settle on to a glass slide, while the liquid was carefully siphoned off, leaving fibres well dispersed on the slide. The slide was examined in an optical microscope and aspect ratio measurements were made on photographs taken in the microscope.

It was clear from the microstructures (see below) that the composites contained some porosity. An attempt was made to quantify this using precision Archimedeian densitometry. The weighing arrangement is illustrated in Fig. 3. A fluorocarbon ("Flutec PP9") was used as the immersion fluid, this being a dense, stable, low surface tension, low vapour pressure liquid at room temperature. The specimens were weighed (to  $\pm 10 \mu\text{g}$ ) in air before and after coating in lacquer, and then immersed in the fluid. The coating was used to eliminate the possibility of the fluid entering any surface-connected porosity. The density,  $\rho$ , of the specimen is given from the recorded weights,  $W$ , by

$$\rho = W_a \left[ \left( \frac{W_{ca} - W_{cl}}{\rho_l - \rho_a} \right) - \left( \frac{W_{ca} - W_{ua}}{\rho_c - \rho_a} \right) \right]^{-1} - \rho_a \quad (1)$$

where the subscripts a, l, u, and c refer, respectively, to air, liquid, uncoated and coated or coating. The porosity can then be deduced from the densities of matrix and fibre and the fibre volume fraction.

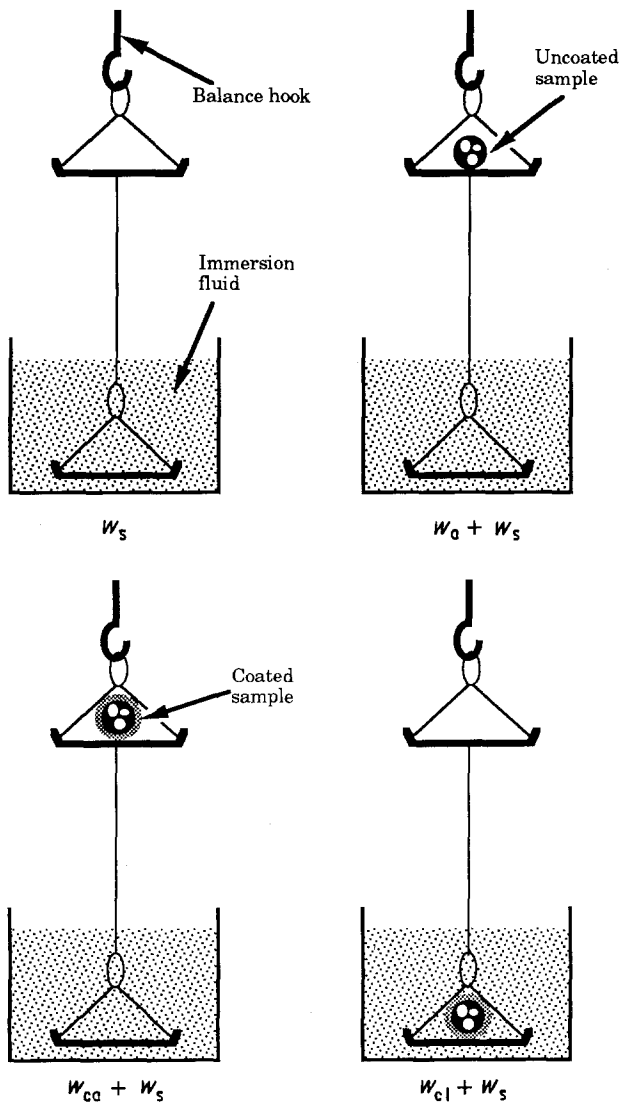


Figure 3 Suspension system for densitometry.

### 3. Results

#### 3.1. Microstructural features

Optical micrographs are shown in Figs 4 and 5 for 14 and 30 vol % fibre contents. Fibre alignment is evident in both cases, although the fibres have been broken up into short lengths. It is also clear that there is considerable porosity present, particularly for the higher fibre content. This porosity shows a strong tendency to be elongated in the extrusion direction, and has a higher effective aspect ratio than the fibres. The porosity tends to form in local regions where fibres are congregated. A clearer impression of the degree of fibre alignment can be obtained from the deep-etched structures shown in Fig. 6 for the 30% fibre material. Although it is possible that there is some preferential retention of slightly longer and hence better aligned fibres, it is clear that the degree of alignment is good.

The fibre aspect ratio distributions were found to follow a fairly smooth curve, with little obvious difference between the composites. A typical histogram is shown in Fig. 7. Generally these gave a number average value of about 2 and a volume average of about 4. Measurements of porosity content revealed that the levels were indeed relatively high, being almost equal to the fibre content for the 14% fibre composite, but nearer to about half of the fibre content for the others. Variations of several per cent were found between measurements from different samples of the same composite.

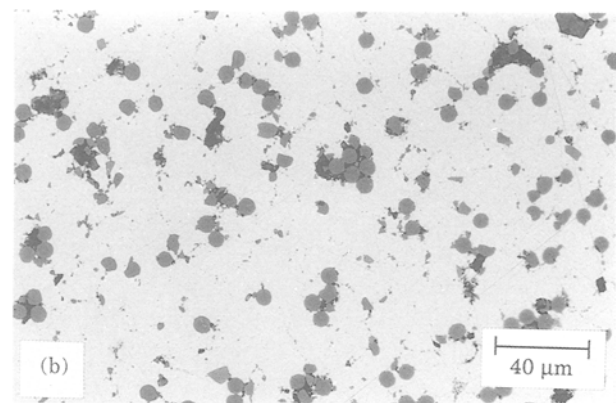
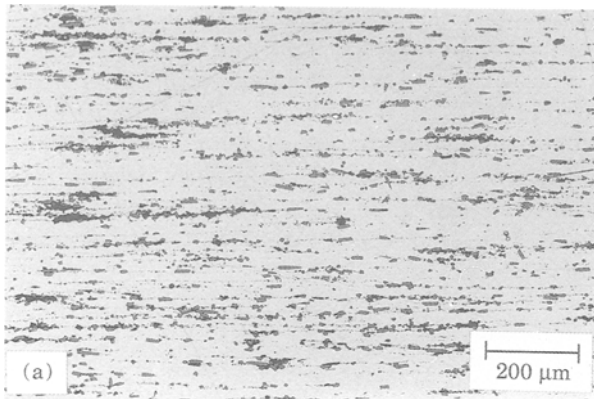


Figure 4 Optical micrographs of the Cu-14 vol % C fibre composite, showing (a) axial and (b) transverse sections.

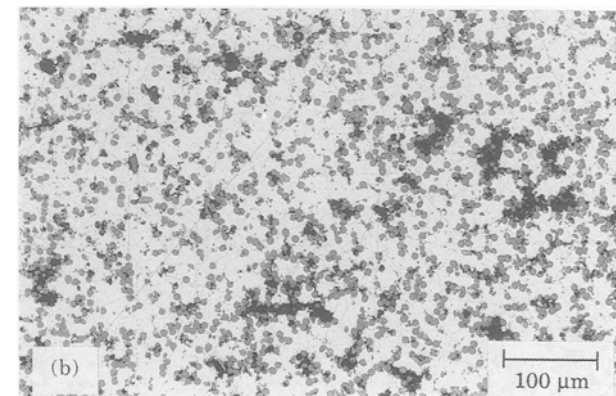
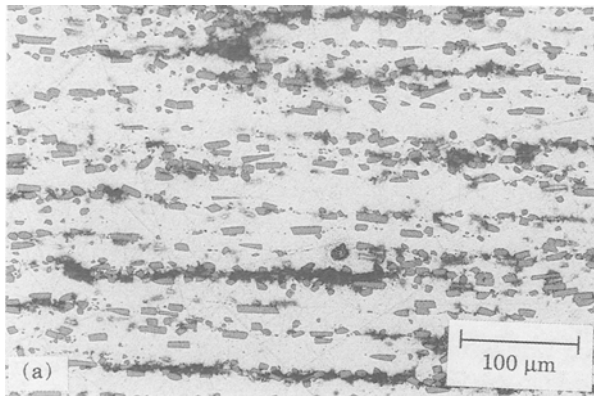


Figure 5 Optical micrographs of the Cu-30 vol % C fibre composite, showing (a) axial and (b) transverse sections.

#### 3.2. Resistivity data

Measured values of composite resistivity in axial and transverse directions are plotted in Fig. 8 as a function of fibre content. These data are presented together with predicted curves from the Eshelby model. Discrepancies between theory and experiment are discussed below.

### 4. Discussion

It is obviously necessary to consider the experimental data in the light of model predictions. The Eshelby method is used here with the mean field approximation [15] for sampling by an inclusion (fibre) of the background current density due to the disturbance of the matrix potential field arising from the presence of neighbouring inclusions. The method is then applicable to non-dilute composites and the appropriate tensor expression for the composite conductivity is

$$\sigma_C = \{(\sigma_M)^{-1} + f[(\sigma_M - \sigma_I)[S - f(S - I)] - \sigma_M]^{-1}(\sigma_I - \sigma_M)(\sigma_M)^{-1}\}^{-1} \quad (2)$$

where  $\sigma$  is conductivity, the subscripts C, M and I refer to composite, matrix and inclusion,  $f$  is the volume fraction of inclusions,  $I$  is the identity tensor and  $S$ , the Eshelby tensor, is dependent only on the ratio of major to minor axis,  $s$ , of the inclusion. The principal values of the resistivity are readily obtained as the reciprocals of the conductivities.

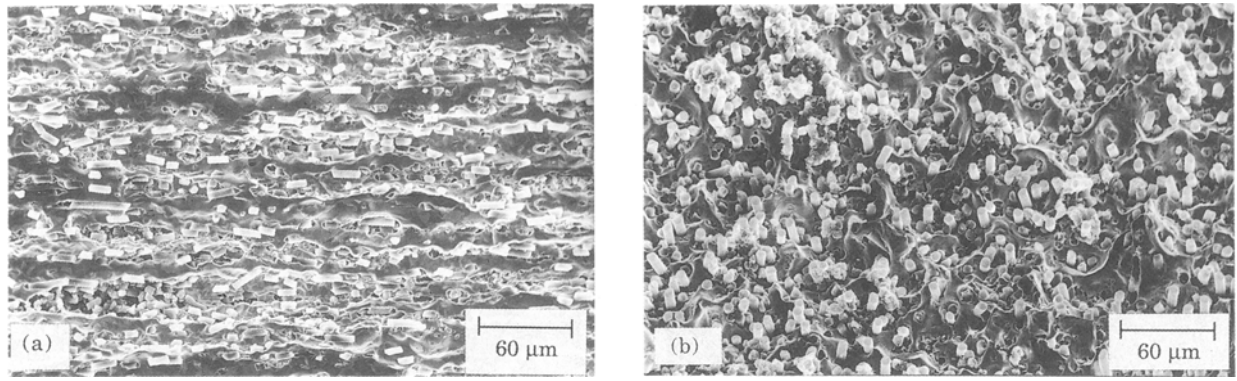


Figure 6 Scanning electron micrographs of the Cu-30 vol % C fibre composite after deep etching, showing (a) axial and (b) transverse sections.

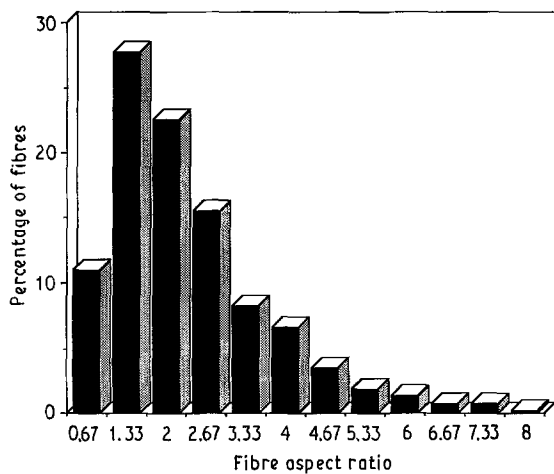


Figure 7 Histogram of fibre aspect ratio values, obtained for a Cu-14 vol % C fibre composite from about 500 fibres.

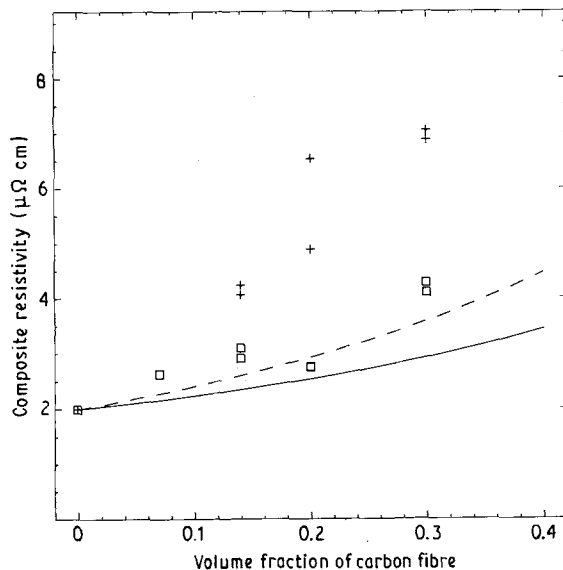


Figure 8 Experimental data and predictions from the Eshelby model for the electrical resistivity as a function of fibre content, using the measured mean fibre aspect ratio value of 4. Predicted curves were obtained using a constant matrix resistivity of  $2 \mu\Omega \text{ cm}$ . (—)  $s = 4$  axial, (---)  $s = 4$  transverse, ( $\square$ ) experimental axial, ( $+$ ) experimental transverse.

The predictions shown in Fig. 8 were obtained using an aspect ratio of 4, corresponding to the measured volume average. Although a range of values were observed in practice, Takao *et al.* [16] have shown

that the Eshelby method should be quite accurate when the volume average value is used, provided the distribution is not grossly skewed or bimodal. It can, however, be seen that agreement in Fig. 8 between theory and experiment is rather poor, the experimental points being both higher than predicted and with a greater difference between axial and transverse values.

The theoretical curves shown in Fig. 8 are based on the matrix being isotropic and having a resistivity equal to that measured for unreinforced copper ( $2.0 \mu\Omega \text{ cm}$ ). One problem with this assumption is that the presence of the fibres affects the microstructure of the matrix, tending to induce higher dislocation densities [17] and a finer grain size. Such microstructural changes have the effect of raising the resistivity of the matrix [18, 19]. The increase is largely attributable to the formation of excess vacancies (and interstitials), with dislocations themselves having only a very small effect [19, 20], but these changes, often together with a refinement of the grain size, tend to be induced simultaneously, notably by plastic deformation. For small strains, the change in resistivity of pure copper as a result of plastic deformation has been reported [18] to obey the equation

$$\Delta\rho = a\varepsilon^p \quad (3)$$

where  $\varepsilon$  is the plastic strain (%),  $a$  is a constant ( $\sim 0.1 \mu\Omega \text{ cm}$  for copper polycrystals) and the exponent  $p$  has a value of about 1.2–1.5. It is not simple to estimate the effective volume-averaged plastic strain in the matrix of a short fibre composite as a result of differential thermal contraction, but the misfit strain ( $\Delta\alpha\Delta T$ ) could be used as an upper limit for high volume fractions of fibre. In the present case, taking  $\Delta T$  as the cooling interval from the extrusion temperature, the axial misfit strain would be of the order of 1%. Hence the maximum change in  $\rho$  on this basis would be about  $0.1 \mu\Omega \text{ cm}$  (i.e. around 5% of its value). In fact, this is almost certainly an overestimate, as experimental measurements [19, 21] of the rise in the resistivity of pure copper with increasing degree of cold work indicate that this levels out at about 4% of the initial resistivity after large reductions (plastic strains  $\geq 50\%$ ).

It may be concluded that an increase in matrix resistivity cannot be invoked to explain the observed

behaviour. In any event, it is clear that this would not explain the large differences between axial and transverse values. This implies that the matrix is inherently anisotropic. An obvious cause of this, and of the high values, is the presence of the porosity, which is markedly elongated in the extrusion direction. The pores can be treated by the Eshelby method as a further set of inclusions, in addition to the carbon fibres; the net result of an attempt to model the effect of both pores ( $s = 10$ ) and fibres ( $s = 4$ ) being present is shown in Fig. 9. In these predictions the pores were taken to have an aspect ratio of 10 and to occupy a volume fraction equal to 80% of that of the fibres, broadly in line with the densitometry measurements. Although these approximations are all very crude, the agreement between theory and experiment is now much better. It seems likely that the remaining discrepancies can be attributed to variations in porosity content.

This does suggest that it should be possible to model the resistivity of such composites fairly successfully without the complication of effects such as electron scattering at interfaces (suggested by Abukay *et al.* [12]), which would be difficult to predict, or the uncertainties concerning the *in situ* dislocation densities. It is possible that the data of Abukay *et al.* could also be explained in terms of an effective anisotropy of matrix resistivity, although in their case it seems likely in view of the matrix and manufacturing route (winding of thin aluminium ribbons around boron fibres, followed by pressing) that aligned oxide films, rather than porosity, were responsible for this anisotropy.

In practical terms, porosity can be eliminated by suitable improvements to processing routes; the results presented here indicate that the resistivities would then be significantly closer to that of the unreinforced matrix. A programme is now planned in which measurements on porosity-free composites should give

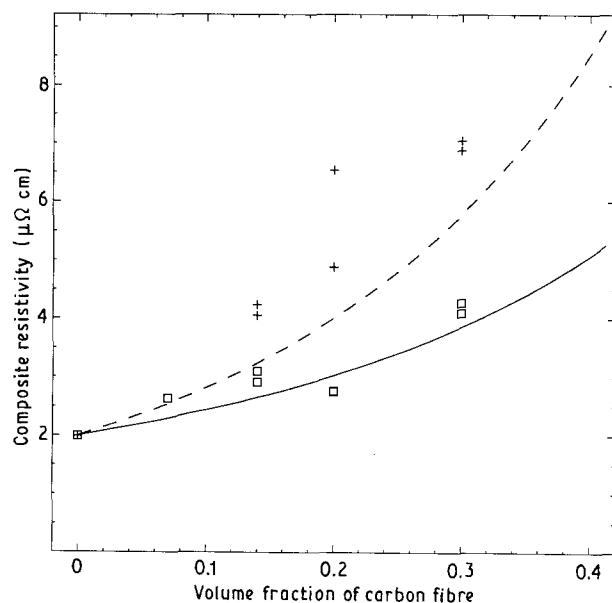


Figure 9 As for Fig. 8, with the additional change in matrix resistivity produced by the presence of pores of aspect ratio 10 (aligned in the same direction as the fibres) and occupying a volume fraction equal to 80% of that of the fibres. (—)  $s = 4$  (+ pores,  $s = 10$ ) axial, (---)  $s = 4$  (+ pores,  $s = 10$ ) transverse, (□) experimental axial, (+) experimental transverse.

more quantitative information about the role of *in situ* matrix microstructure. This will include measurements made before and after *in situ* recrystallization of the matrix, in order to verify the suggestion that atomic scale defects and grain boundaries do not play a very significant role.

## 5. Conclusions

Composites of short carbon fibres in a copper matrix have been made by a powder blending and extrusion route and measurements made of their axial and transverse electrical resistivities. For this system, the fibres are, in effect, non-conductors. The following conclusions have been drawn from these data and from microstructural observations.

1. The axial and, particularly, the transverse resistivities were found to rise with fibre content at a greater rate than that predicted by the Eshelby equivalent inclusion method on the basis of a matrix resistivity equal to that of unreinforced copper and a mean fibre aspect ratio of 4 (the measured value).

2. This effect might have been partially attributed to an increased matrix resistivity caused by a high content of dislocations and other defects, which result from differential thermal contraction strains generated during post-fabrication cooling. However, this is not expected to effect a very significant increase in matrix resistivity and in any event it cannot account for the large difference between axial and transverse values.

3. It is proposed that the *in situ* matrix resistivity was effectively raised and rendered anisotropic by the presence of elongated pores. A suitable adaptation of the Eshelby method has been used to predict the effect of this and has been found to give fairly good agreement with experiment. It has not been necessary to invoke effects suggested by other workers, such as electron scattering at fibre/matrix boundaries, which is probably not very significant in metal matrix composites.

## Acknowledgements

The authors thank Mr K. Page, Materials Science Department, Cambridge, for his valuable help with the electrical measuring system, Mr K. Gray of the same department, for assistance in preparing the composites, Mr H. Greenwood, Courtaulds Ltd, Coventry, for advice concerning fibre properties, and Mr A. Forno, NPL, Teddington, for carrying out the extrusion operations.

## References

1. D. K. HALE, *J. Mater. Sci.* **11** (1976) 2105.
2. L. E. NIELSEN, *Ind. Engng Chem. Fundam.* **13** (1974) 17.
3. Y. BENVENISTE, *J. Appl. Phys.* **61** (1987) 2840.
4. D. P. H. HASSELMAN and L. F. JOHNSON, *J. Comp. Mater.* **21** (1987) 508.
5. J. E. SCHOUTENS and F. S. ROIG, *J. Mater. Sci.* **22** (1987) 181.
6. H. HATTA and M. TAYA, *Int. J. Engng Sci.* **24** (1986) 1159.
7. *Idem*, *J. Appl. Phys.* **59** (1986) 1851.
8. M. TAYA, in "Proceedings of the 9th Risø International Symposium on Mechanical and Physical Behaviour of

- Metallic and Ceramic Composites", edited by S. I. Andersen *et al.* (1988) pp. 201–31.
9. B. J. LAST and D. J. THOULESS, *Phys. Rev. Lett.* **27** (1971) 1719.
  10. M. TAYA and N. UEDA, *Trans ASME J. Engng Matter. Technol.* **109** (1987) 252.
  11. A. J. REEVES, R. TAYLOR and T. W. CLYNE, *Mater. Sci. Engng* (1991) in press.
  12. D. ABUKAY, K. V. RAO and S. ARAJS, *Fibre Sci. Technol.* **10** (1977) 313.
  13. K. KUNIYA, H. ARAKAWA, T. KANANI and A. CHIBA, *Trans. Jpn Inst. Metals* **28** (1987) 819.
  14. S. DeBONDT, L. FROYEN and A. DERUYTTERE, in "Proceedings of the 9th Risø International Symposium on Mechanical and Physical Behaviour of Metallic and Ceramic Composites", edited by S. I. Andersen *et al.* (1988) pp. 345–48.
  15. K. TANAKA and T. MORI, *Acta Metall.* **18** (1970) 931.
  16. Y. TAKAO, T. W. CHOU and M. TAYA, *J. Appl. Mech.* **104** (1982) 536.
  17. R. J. ARSENAULT and M. TAYA, *Acta Metall.* **35** (1987) 651.
  18. H. G. van BUEREN, *Z. Metallkde* **46** (1955) 272.
  19. D. K. CRAMPTON, H. L. BURGHOFF and G. T. STACEY, *Trans. AIME* **143** (1941) 228.
  20. J. K. STANLEY, "Electrical and Magnetic Properties of Metals" (ASM, Ohio, 1963).
  21. R. BARDENHAUER and H. SCHMIDT, *Mitt. Kaiser Wilhelm Inst. Eisenforschung* **10** (1928) 193.

*Received 24 September 1990  
and accepted 18 March 1991*